Available online at www.sciencedirect.com
ScienceDirect
Mendeleev Commun., 2022, **32**, 807–809

Mendeleev Communications

In situ FTIR study of surface site transformations in $Pd_3In/\alpha\text{-}Al_2O_3$ and $Pd_3Ag/\alpha\text{-}Al_2O_3$ induced by CO adsorption

**Nadezhda S. Smirnova,[a] Galina N. Baeva,[a] Pavel V. Markov,[a] Igor S. Mashkovsky,[a]
Andrey V. Bukhtiyarov,[b] Yan V. Zubavichus[b] and Alexander Yu. Stakheev*[a]**

[a] *N. D. Zelinsky Institute of Organic Chemistry, Russian Academy of Sciences, 119991 Moscow, Russian Federation. Fax: +7 499 135 5328; e-mail: st@ioc.ac.ru*
[b] *G. K. Boreskov Institute of Catalysis, Siberian Branch of the Russian Academy of Sciences, 630090 Novosibirsk, Russian Federation*

DOI: 10.1016/j.mencom.2022.11.033

In the course of the treatment of $Pd_3Ag/\alpha\text{-}Al_2O_3$ in 0.5%CO + He at 200 °C, intense transformation of single atom Pd_1 surface sites isolated from each other by Ag atoms to multiatomic Pd_n ($n \geqslant 2$) ensembles occurs, as revealed by a rapid increase in the intensity of multibonded CO bands in FTIR spectra. The structure of intermetallic Pd_3In nanoparticles is significantly more stable, and the formation of new multiatomic adsorption centers was not observed even after extended CO exposures.

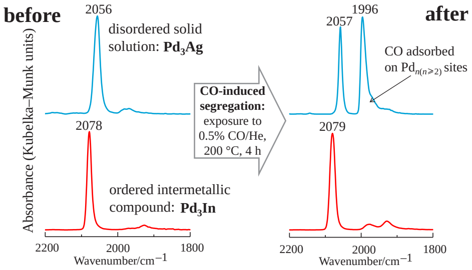

Keywords: adsorbate-induced segregation, Pd–Ag solid solution, palladium-based alloy, Pd–In intermetallics, DRIFT spectroscopy of adsorbed CO.

Bimetallic palladium-based catalysts are widely used in chemical processes since the presence of a second element improves their catalytic performance in comparison with monometallic Pd.[1,2] When Pd is alloyed with an inactive or less active metal (Ag, Au, Zn, and In), the catalyst selectivity is often improved by diluting Pd ensembles and reducing their size down to single-atom Pd_1 sites isolated from each other by inactive metal atoms (single atom alloy catalysts, SAA). Such catalysts demonstrate outstanding selectivity due to uniformity of isolated Pd_1 sites and prevention of multipoint adsorption of reacting molecules in accordance with the active-site isolation concept.[3]

The surface composition and the structure of active sites can be significantly affected upon adsorption of reacting molecules in the course of adsorbate-induced surface segregation due to enrichment of the surface with metal atoms having a higher binding energy with the adsorbate.[4] The surface segregation processes can significantly change the catalytic performance of bimetallic catalysts by a considerable rearrangement of the geometry of active sites. For example, it was demonstrated that the fraction of Pd atoms on the surface of Pd–Cu,[5] Pd–Ag,[6,7] or Pd–Au[8,9] can be significantly enhanced by CO or acetylene adsorption.

The enrichment of a Pd–M surface in Pd improves the catalyst activity in the selective gas-phase hydrogenation of acetylene in acetylene–ethylene mixtures and the liquid-phase hydrogenation of terminal and internal alkynes.[4,5,10,11] On the other hand, it favors the transformation of isolated Pd_1 atoms to multiatomic $Pd_{n(n \geqslant 2)}$ ensembles, which can negatively affect selectivity.[5] Therefore, it is important to impede adsorbate-induced segregation and prevent the formation of multiatomic Pd_n centers for preserving catalyst selectivity.

The tendency of Pd alloy to undergo adsorbate-induced segregation depends on the second metal and the bimetallic crystal structure. Substitutional alloys Pd–M (M = Cu, Ag, Au, *etc.*) are prone to the surface segregation of a second metal in a vacuum or an inert atmosphere[12] and the surface segregation of Pd induced by chemisorption of molecules with high adsorption energy on palladium.[7] On the other hand, there are several indications that intermetallic Pd surface possesses much higher stability against segregation[13,14] due to the covalent bonding, ordered crystal structure, and significantly higher enthalpy of formation (~60 kJ mol^{-1} for Pd–In[15]).

Unfortunately, comparative studies of the surface stability of intermetallic and substitutional solid solution nanoparticles upon adsorption are scarce. In many studies, the adsorbate-induced surface segregation was investigated by XPS spectroscopy,[6,16] which does not provide detailed information on the structure of surface sites since it collects averaged data over several surface layers (up to 5 nm depth). FTIR CO spectroscopy can be convenient to characterize Pd–M surface sites due to the adsorption of CO on Pd atoms only in a top surface layer. Therefore, this work was focused on studying the transformation of surface sites in intermetallic (Pd_3In), and substitutional solid solution (Pd_3Ag) nanoparticles upon CO adsorption using *in situ* FTIR spectroscopy.

In this study, we used conventional $Pd_3In/\alpha\text{-}Al_2O_3$ and $Pd_3Ag/\alpha\text{-}Al_2O_3$ catalysts and a reference sample (3% Pd/$\alpha\text{-}Al_2O_3$) instead of model Pd–In/HOPG (highly oriented pyrolytic graphite) samples considered previously.[16] The samples were characterized by TEM, XRD, and FTIR CO analysis (see Online Supplementary Materials for experimental details and results of TEM and XRD analysis).

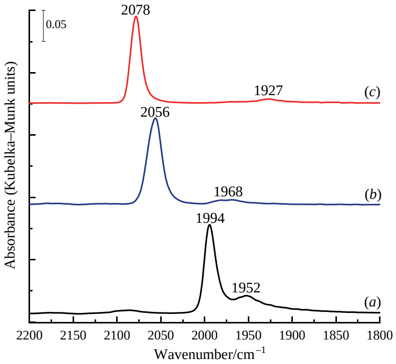

Figure 1 DRIFT spectra of adsorbed CO on (*a*) freshly reduced Pd/α-Al_2O_3 (reference sample), (*b*) Pd_3Ag/α-Al_2O_3, and (*c*) Pd_3In/α-Al_2O_3 catalysts.

Figure 1 shows the DRIFT spectra of adsorbed CO for all samples. The FTIR CO spectrum of Pd/α-Al_2O_3 is predominated by a broad absorption band at 1994 cm^{-1} and a shoulder at 1952 cm^{-1}. According to Agostini *et al.*,[17] these bands are attributable to the bridged and threefold bridged CO adsorbed on Pd_2 and Pd_3 sites, respectively. The band intensity corresponding to the CO adsorbed linearly on top of Pd atom (2100–2080 cm^{-1}) is very low. The predominance of multipoint CO adsorption is explained by the fact that, on a monometallic Pd surface, CO preferentially adsorbs on Pd_3 hollow sites or two neighboring Pd atoms as the energy of adsorption on these sites is more favorable than the linear adsorption of CO on single Pd atom: 163, 142, and 111 kJ mol^{-1}, respectively.[18]

The FTIR spectrum of the reduced Pd_3Ag sample shows an intense band at about 2056 cm^{-1} characteristic of CO adsorbed linearly on Pd atom [Figure 1(*b*)]. The band intensity of bridged CO (at ~1968 cm^{-1}) is essentially negligible indicating the predominance of Pd_1 centers isolated by Ag atoms and admitting only linear CO adsorption. Multiatomic Pd_n centers, where two- and three-coordination of CO is possible, are essentially absent, as indicated by a marginal intensity of bands within a range of 2000–1820 cm^{-1}. The shift of a linear CO band toward lower wavenumbers (2056 *vs*. 2080–2095 cm^{-1} in the spectrum of monometallic Pd[19]) can be related to a charge redistribution between Pd and Ag atoms and to a decrease in the lateral interaction between adsorbed CO molecules.

These results are in good agreement with previous data for catalysts with different Pd : Ag ratios.[10] It was shown that Pd_1 sites isolated from each other by Ag atoms predominate on the surface of Pd_xAg_y nanoparticles even in the samples with high Pd : Ag ratios as a result of surface segregation of Ag. The enrichment of the surface with Ag atoms is explained by an energy gain due to the surface segregation of Ag in Pd–Ag alloy (25 kJ mol^{-1}) caused by the lower surface energy of Ag.[20]

The spectrum of CO adsorbed on intermetallic Pd_3In sample is also predominated by an absorption band at 2078 cm^{-1} attributable to CO linearly adsorbed on top of Pd atom, while the band intensity at 1927 cm^{-1} ascribed to triple bridge-bonded CO at a hollow site on the Pd_3In (111) surface is marginal.[21] The low intensity of the triple bridge-bonded CO band can be related to the formation of the most thermodynamically stable Pd_1In_1 intermetallic compound on the surface and subsurface layers of PdIn nanoparticles, as it was shown for Pd_xIn_y/SiO_2.[22] It was demonstrated that the specific geometric arrangement of Pd and In atoms on the surface of PdIn intermetallic compound (IMC) prevents bridged and hollow-bonded CO adsorption.[23]

Thus, a comparison of FTIR CO data for monometallic and bimetallic samples clearly evidenced that neither Pd_3Ag nor Pd_3In samples show a tendency to multiple coordination of adsorbed CO, which indicates that their surface is dominated by Pd_1 sites capable of only linear CO adsorption, while the fraction of multiatomic Pd_n ($n \geqslant 2$) ensembles is negligible.

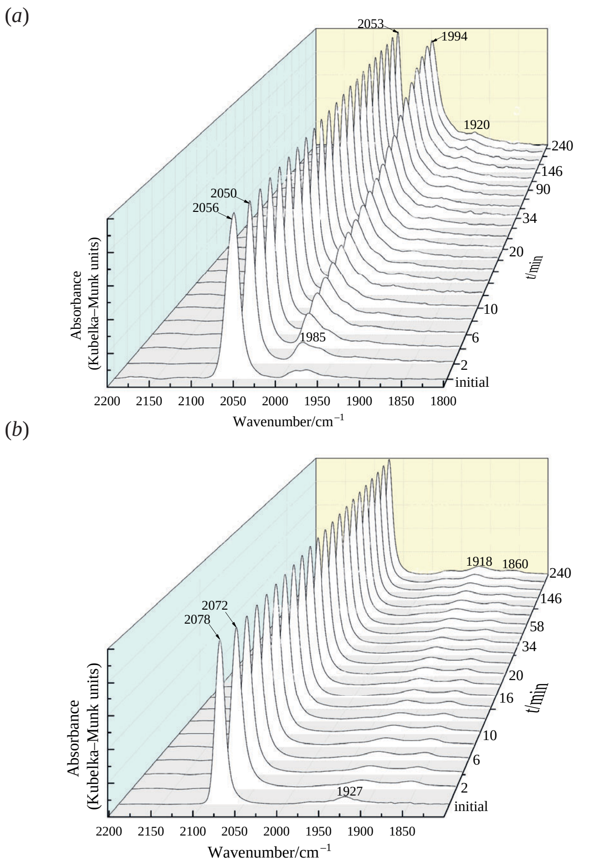

Figure 2 Dynamics of CO-induced segregation of (*a*) Pd_3Ag/Al_2O_3 and (*b*) Pd_3In/Al_2O_3 catalysts (200 °C, 4 h, 0.5% CO/He flow). The DRIFT CO spectrum of the initial sample was recorded at 50 °C.

To compare the stability of two bimetallic systems under conditions of adsorbate-induced segregation, the Pd_3Ag and Pd_3In samples were treated in a flow of 0.5% CO/He at 200 °C for 4 h (Figure 2). The treatment of the Pd_3Ag sample in CO led to a gradual increase in the intensity of the bridge-bonded CO peak and its shift from 1985 to 1994 cm^{-1} closer to the bridge-bonded CO band in monometallic palladium.[24,25] After ~20–30 min, a shoulder at 1920 cm^{-1}, which is characteristic of triple bridge-bonded CO at a hollow Pd_3 site,[26] appeared. The appearance and growth of the intensity of these bands indicated the transformation of Pd_1 sites to Pd_n ensembles enabling multipoint CO adsorption due to segregation of Pd.[5,19]

In contrast to the Pd_3Ag solid solution, the influence of CO on the surface structure of the Pd_3In intermetallic nanoparticles is marginal. The position of a linear CO adsorption band (2072 cm^{-1}) remained unchanged within 4 h of the experiment. During the first few minutes of CO treatment, a minor transformation of the multiply coordinated CO bands (2000–1820 cm^{-1}) and the appearance of peaks at 1918 and 1860 cm^{-1} were observed. These absorption bands can be explained by the presence of hcp2 centers on the surface of Pd_3In IMC, which are favorable for the adsorption of hollow-bonded CO.[21] However, the integral intensity of the multiply coordinated CO bands is marginal, and it remains almost constant in the course of CO exposure.

It is informative to qualitatively analyze the dynamics of bridged CO intensity changes related to the formation of multiatomic Pd ensembles on the surface of Pd_3Ag and Pd_3In nanoparticles. Figure 3 shows the dependence of the $I_{Br}/(I_{Lin} + I_{Br})$ intensity ratio on the duration of the CO treatment. For the Pd_3Ag sample, we can observe a rapid increase in the $I_{Br}/(I_{Lin}+I_{Br})$ ratio in the first 30–40 min. As was previously

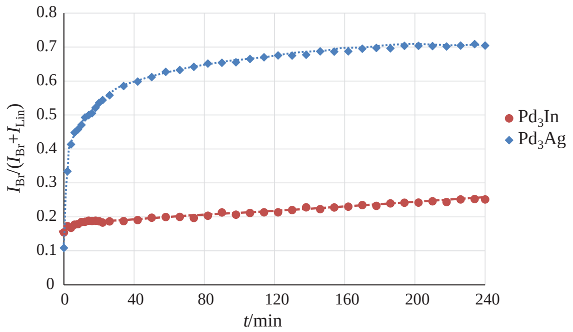

Figure 3 Dependence of the intensity ratio of bridged and linear CO forms on the exposure time in a CO-containing gas flow.

shown on Ag/PdAg/Ag(111) and $Pd_{75\%}Ag_{25\%}(100)$ models, such systems are characterized by the formation of structures with palladium atoms located in the near-surface (two to three outmost layers) region of the catalyst.[6,27] This structure is very sensitive to environmental conditions; therefore, an exposure to CO leads to the rapid segregation of near-surface palladium atoms on the catalyst surface. Presumably, a further decrease in the rate of segregation is associated with the suppressed diffusion of palladium atoms from the bulk of the bimetallic particle because the activation barrier for bulk diffusion is much higher.[6]

In contrast to the Pd_3Ag catalyst, the intermetallic Pd_3In sample showed only minor changes during the experiment. The lower tendency of Pd segregation is explained due to a larger strength of the Pd–In bond, more covalent bonding between Pd and In, and the suppressed diffusion of palladium through the ordered Pd_3In structure. In the case of Pd_3In, small structural changes on the surface can be associated with a strong interaction between CO and palladium atoms, which favors the segregation of palladium on the surface in contrast to In-rich Pd_1In_1 IMC.[21] Note that no changes were found on the surface of Pd–In/HOPG during CO-induced segregation.[16] This can be explained by both the milder experimental conditions (100–150 °C, 1h)[16] and the fact that XPS provides information from several layers up to 5 nm deep.

It is remarkable that the observed changes in the surface structure of Pd_3In and Pd_3Ag catalysts are entirely reversible. It was found that reductive treatment in hydrogen at 500 °C completely restored the initial structure (see Figure S3 in Online Supplementary Materials).

The results of this study indicated that the treatment of Pd_3Ag solid solution nanoparticles with CO induced fundamental changes in their surface structure, as indicated by the appearance of numerous multiatomic $Pd_{n(n \geqslant 2)}$ ensembles, which significantly affect catalytic functions. In contrast to Pd_3Ag, the surface structure of intermetallic Pd_3In nanoparticles demonstrated high stability and no pronounced tendency to transform Pd_1 sites of linear CO adsorption into multiatomic Pd_n centers enabling multipoint CO adsorption.

This work was supported by the Russian Science Foundation (grant no. 19-13-00285-P). The authors are grateful to the Department of Structural Studies at N. D. Zelinsky Institute of Organic Chemistry of the Russian Academy of Sciences for the TEM characterization of samples.

Online Supplementary Materials

Supplementary data associated with this article can be found in the online version at doi: 10.1016/j.mencom.2022.11.033.

References

1 T. D. Shittu and O. B. Ayodele, *Front. Chem. Sci. Eng.*, 2022, **16**, 1031.
2 I. A. Chetyrin, A. V. Bukhtiyarov, I. P. Prosvirin and V. I. Bukhtiyarov, *Mendeleev Commun.*, 2021, **31**, 635.
3 H. Verbeek and W. M. H. Sachtler, *J. Catal.*, 1976, **42**, 257.
4 M. A. Panafidin, A. V. Bukhtiyarov, I. P. Prosvirin, I. A. Chetyrin, A. Yu. Klyushin, A. Knop-Gericke, N. S. Smirnova, P. V. Markov, I. S. Mashkovsky, Y. V. Zubavichus, A. Yu. Stakheev and V. I. Bukhtiyarov, *Appl. Surf. Sci.*, 2022, **571**, 151350.
5 A. J. McCue and J. A. Anderson, *J. Catal.*, 2015, **329**, 538.
6 M. A. van Spronsen, K. Daunmu, C. R. O'Connor, T. Egle, H. Kersell, J. Oliver-Meseguer, M. B. Salmeron, R. J. Madix, P. Sautet and C. M. Friend, *J. Phys. Chem. C*, 2019, **123**, 8312.
7 E. Vignola, S. N. Steinmann, K. L. Mapihan, B. D. Vandegehuchte, D. Curulla and P. Sautet, *J. Phys. Chem. C*, 2018, **122**, 15456.
8 A. V. Bukhtiyarov, I. P. Prosvirin, A. A. Saraev, A. Yu. Klyushin, A. Knop-Gericke and V. I. Bukhtiyarov, *Faraday Discuss.*, 2018, **208**, 255.
9 M. Luneau, E. Guan, W. Chen, A. C. Foucher, N. Marcella, T. Shirman, D. M. A. Verbart, J. Aizenberg, M. Aizenberg, E. A. Stach, R. J. Madix, A. I. Frenkel and C. M. Friend, *Commun. Chem.*, 2020, **3**, 46.
10 A. V. Rassolov, G. O. Bragina, G. N. Baeva, N. S. Smirnova, A. V. Kazakov, I. S. Mashkovsky, A. V. Bukhtiyarov, Ya. V. Zubavichus and A. Yu. Stakheev, *Kinet. Catal.*, 2020, **61**, 758 (*Kinet. Katal.*, 2020, **61**, 676).
11 A. V. Rassolov, P. V. Markov, G. O. Bragina, G. N. Baeva, I. S. Mashkovskii, I. A. Yakushev, M. N. Vargaftik and A. Yu. Stakheev, *Kinet. Catal.*, 2016, **57**, 853 (*Kinet. Katal.*, 2016, **57**, 865).
12 A. V. Ruban, H. L. Skriver and J. K. Nørskov, in *Surface Alloys and Alloy Surfaces*, ed. D. P. Woodruff, Elsevier, 2002, vol. 10, pp. 1–29.
13 M. Armbrüster, *Sci. Technol. Adv. Mater.*, 2020, **21**, 303.
14 K. Kovnir, M. Armbrüster, D. Teschner, T. V. Venkov, L. Szentmiklósi, F. C. Jentoft, A. Knop-Gericke, Y. Grin and R. Schlögl, *Surf. Sci.*, 2009, **603**, 1784.
15 D. El Allam, M. Gaune-Escard, J.-P. Bros and E. Hayer, *Metall. Mater. Trans. B*, 1995, **26**, 767.
16 A. Yu. Fedorov, A. V. Bukhtiyarov, M. A. Panafidin, I. P. Prosvirin, I. A. Chetyrin, N. S. Smirnova, P. V. Markov, Y. V. Zubavichus, A. Yu. Stakheev and V. I. Bukhtiyarov, *Nano-Struct. Nano-Objects*, 2022, **29**, 100830.
17 G. Agostini, R. Pellegrini, G. Leofanti, L. Bertinetti, S. Bertarione, E. Groppo, A. Zecchina and C. Lamberti, *J. Phys. Chem. C*, 2009, **113**, 10485.
18 I. V. Yudanov, R. Sahnoun, K. M. Neyman, N. Rösch, J. Hoffmann, S. Schauermann, V. Johanek, H. Unterhalt, G. Rupprechter, J. Libuda and H.-J. Freund, *J. Phys. Chem. B*, 2003, **107**, 255.
19 A. Yu. Stakheev, N. S. Smirnova, P. V. Markov, G. N. Baeva, G. O. Bragina, A. V. Rassolov and I. S. Mashkovsky, *Kinet. Catal.*, 2018, **59**, 610 (*Kinet. Katal*., 2018, **59**, 601).
20 A. V. Ruban, H. L. Skriver and J. K. Nørskov, *Phys. Rev. B*, 1999, **59**, 15990.
21 R. Zhang, M. Peng, L. Ling and B. Wang, *Chem. Eng. Sci.*, 2019, **199**, 64.
22 Z. Wu, E. C. Wegener, H.-T. Tseng, J. R. Gallagher, J. W. Harris, R. E. Diaz, Y. Ren, F. H. Ribeiro and J. T. Miller, *Catal. Sci. Technol.*, 2016, **6**, 6965.
23 N. S. Smirnova, I. S. Mashkovsky, P. V. Markov, A. V. Bukhtiyarov, G. N. Baeva, H. Falsig and A. Y. Stakheev, *Catalysts*, 2021, **11**, 1376.
24 S. Schauermann, J. Hoffmann, V. Johanek, J. Hartmann, J. Libuda and H.-J. Freund, *Angew. Chem., Int. Ed.*, 2002, **41**, 2532.
25 K. Wolter, O. Seiferth, H. Kuhlenbeck, M. Baumer and H.-J. Freund, *Surf. Sci.*, 1998, **399**, 190.
26 T. Lear, R. Marshall, J. A. Lopez-Sanchez, S. D. Jackson, T. M. Klapötke, M. Bäumer, G. Rupprechter, H.-J. Freund and D. Lennon, *J. Chem. Phys.*, 2005, **123**, 174706.
27 M. D. Strømsheim, I.-H. Svenum, M. Mahmoodinia, V. Boix, J. Knudsen and H. J. Venvik, *Catal. Today*, 2022, **384–386**, 265.

Received: 2nd June 2022; Com. 22/6921